NEUROSCIENCE
RESEARCH ARTICLE

B. La Scaleia et al. / Neuroscience 510 (2023) 32–48

Enhancement of Vestibular Motion Discrimination by Small Stochastic Whole-body Perturbations in Young Healthy Humans

Barbara La Scaleia, [a] **Francesco Lacquaniti** [b,c] **and Myrka Zago** [a,d*]

[a] *Laboratory of Visuomotor Control and Gravitational Physiology, IRCCS Fondazione Santa Lucia, 00179 Rome, Italy*

[b] *Laboratory of Neuromotor Physiology, IRCCS Fondazione Santa Lucia, 00179 Rome, Italy*

[c] *Department of Systems Medicine and Center of Space Biomedicine, University of Rome Tor Vergata, 00133 Rome, Italy*

[d] *Department of Civil Engineering and Computer Science Engineering and Center of Space Biomedicine, University of Rome Tor Vergata, 00133 Rome, Italy*

Abstract—Noisy galvanic vestibular stimulation has been shown to improve vestibular perception in healthy subjects. Here, we sought to obtain similar results using more natural stimuli consisting of small-amplitude motion perturbations of the whole body. Thirty participants were asked to report the perceived direction of antero-posterior sinusoidal motion on a MOOG platform. We compared the baseline perceptual thresholds with those obtained by applying small, stochastic perturbations at different power levels along the antero-posterior axis, symmetrically distributed around a zero-mean. At the population level, we found that the thresholds for all but the highest level of noise were significantly lower than the baseline threshold. At the individual level, the threshold was lower with at least one noise level than the threshold without noise in 87% of participants. Thus, small, stochastic oscillations of the whole body can increase the probability of recognizing the direction of motion from low, normally subthreshold vestibular signals, possibly due to stochastic resonance mechanisms. We suggest that, just as the external noise of the present experiments, also the spontaneous random oscillations of the head and body associated with standing posture are beneficial by enhancing vestibular thresholds with a mechanism similar to stochastic resonance.

Key words: vestibular thresholds, imperceptible stimuli, stochastic resonance, direction-recognition, spatial orientation, posture.

INTRODUCTION

By monitoring 3-dimensional angular velocities and gravito-inertial accelerations of the head, the vestibular system contributes to keep clear vision and postural equilibrium (Angelaki and Cullen, 2008). Vestibular information is also critical for the perception of head position and displacement, and therefore for our sense of spatial orientation (Merfeld, 2012). Thus, discriminating forward from backward direction of passive motion in darkness is a spatial orientation task that heavily relies on vestibular cues. The precision of head motion perception can be quantified by means of the psychometric functions for the discrimination of head-centered passive translations and tilts (Merfeld, 2011). The psychometric function yields an estimate of the individual vestibular threshold, that is, of the minimum amount of motion necessary to reliably recognize the direction of motion.

In young persons, vestibular thresholds are generally low, denoting great precision of motion discrimination (for a review, see Diaz-Artiles and Karmali, 2021). The thresholds progressively increase after the age of about 40 years (Kingma, 2005; Roditi and Crane, 2012; Agrawal et al., 2013; Bermúdez Rey et al., 2016). Moreover, there is a correlation between vestibular thresholds and postural stability: higher thresholds tend to be associated with greater postural sway even in young healthy people (Karmali et al., 2021).

Although noise usually represents an undesirable disturbance, there exist specific cases of "good" noise that improve threshold-like systems. Thus, low amplitude noise externally added to muscle spindles (Cordo et al., 1996), cutaneous receptors (Collins et al., 1996a) or vestibular hair cells (Flores et al., 2016) enhances their responses to weak stimuli. Also, low amplitude noise added to visual (Simonotto et al., 1997), auditory (Jaramillo and Wiesenfeld, 1998), tactile

*Correspondence to: Myrka Zago, Laboratory of Visuomotor Control and Gravitational Physiology, IRCCS Fondazione Santa Lucia, 00179 Rome, Italy.
E-mail addresses: b.lascaleia@hsantalucia.it (B. La Scaleia), lacquaniti@med.uniroma2.it (F. Lacquaniti), myrka.zago@uniroma2.it (M. Zago).

Abbreviations: BRGLM, bias-reduced generalized linear model; CV, coefficient of variation; GLM, generalized linear model; GVS, galvanic vestibular stimulation; PEST, parameter estimation by sequential testing; RMS, root-mean-square; SR, stochastic resonance.

https://doi.org/10.1016/j.neuroscience.2022.12.010
0306-4522/

(Collins et al., 1996b) stimuli, or added directly to cortical networks (van der Groen and Wenderoth, 2016) can improve the sensory thresholds. These observations are often interpreted in the context of stochastic resonance (SR).

SR consists in the phenomenon whereby small amplitude, random noise in a nonlinear system enhances detection and transmission of weak signals in the system (Benzi et al., 1982; Gammaitoni et al., 1998). SR predicts that, when using different levels of noise, one obtains a maximum performance at some optimal noise level, and further increases in the noise intensity lead to no enhancement or even degrade the performance (Moss et al., 2004; McDonnell and Abbott, 2009; Galvan-Garza, 2016). The optimal noise level and the extent of performance improvement typically vary across individuals (e.g., Collins et al., 1996b; Mori and Kai, 2002; Wells et al., 2005; Martínez et al., 2007; Mulavara et al., 2011; Iwasaki et al., 2014; Goel et al., 2015; Fujimoto et al., 2016; van der Groen and Wenderoth, 2016; Treviño et al., 2016; Yashima et al., 2021). This inter-subject variability presumably depends on the fact that the noise added by the experimenter (external noise) combines with the electrochemical noise generated within the nervous system (internal noise) to determine the overall amount of noise mixed with the input signal (Mori and Kai, 2002; Treviño et al., 2016). It is the neural noise that can vary substantially as a function of individual factors, such as attention, motivation, fatigue, brain functional organization, etc. (Faisal et al., 2008; Dhawale et al., 2017; Vidal and Lacquaniti, 2021).

Results compatible with SR have been observed also by using low-levels of stochastic galvanic vestibular stimulation (GVS). GVS consists in applying electrical noise to the peripheral vestibular system by means of electrodes placed at the mastoids (Fitzpatrick and Day, 2004; Dlugaiczyk et al., 2019). GVS has been shown to ameliorate vestibular perception (Mulavara et al., 2015; Galvan-Garza et al., 2018; Keywan et al., 2018, 2020a; Wuehr et al., 2018), as well as other vestibular-mediated responses such as ocular counter-rolling (Serrador et al., 2018), balance (Mulavara et al., 2011; Goel et al., 2015; Fujimoto et al., 2016; Keywan et al., 2020a), vestibulo-spinal reflexes (Wuehr et al., 2018), mobility (Putman et al., 2021), locomotion (Mulavara et al., 2015; Iwasaki et al., 2018), and cross-modal visual perception (Voros et al., 2021). Inter-subject variability of optimal GVS noise levels has been shown to be a result of the individual level of vestibular function. Thus, greater noise amplitudes are required for individuals with reduced vestibular function due to aging (Serrador et al., 2018) or bilateral vestibulopathy (Iwasaki et al., 2014). Furthermore, individuals with vestibular hypofunction show greater performance improvements in response to GVS compared to healthy individuals (Iwasaki et al., 2014; Nooristani et al., 2021).

Adding low-amplitude GVS on top of head motion stimuli in young healthy participants can improve the thresholds of motion direction discrimination (Galvan-Garza et al., 2018; Keywan et al., 2018, 2019, 2020a). Some inconsistencies between studies have arisen because of the varying methodologies employed to determine the optimal GVS amplitude, frequency bandwidths, and type of vestibular assay (see Stefani et al., 2020; Voros et al., 2021). Thus, GVS significantly decreased the thresholds for roll-tilt discrimination at 0.2 Hz in one study (Galvan-Garza et al., 2018), whereas it did not significantly affect the thresholds at 0.2 Hz but only at 0.5 Hz and 1 Hz in another study (Keywan et al., 2018). Still another study (Keywan et al., 2019) showed that GVS reduced the thresholds for inter-aural translation of upright participants (stimulating the otoliths) but not the thresholds for yaw-rotation with the head pitched forward 71° (primarily resulting in stimulation of the semicircular canals), suggesting that GVS mainly affects otolith-mediated perception (Zink et al., 1998). However, an electrophysiological study in macaques showed that GVS produces robust and parallel activation of both canal and otolith primary afferents, resulting in constant GVS-evoked neuronal detection thresholds across all afferents (Kwan et al., 2019). This study also showed that afferent tuning differs for GVS versus natural motion stimulation, due to the fact that GVS bypasses the mechano-transduction of both the semicircular canals and the otolith organs, which contribute to the dynamics of vestibular responses to rotation and translation, respectively (Kwan et al., 2019). In fact, GVS directly activates the hair cells and vestibular afferents via electrical transmission (Kwan et al., 2019; Dlugaiczyk et al., 2019).

Given that GVS can elicit unnatural vestibular afferent inputs (Kwan et al., 2019) and can sometimes cause discomfort to the subjects (Utz et al., 2011; Dlugaiczyk et al., 2019), it would be interesting if one was able to enhance head motion discrimination by adding perturbations that resemble natural motion stimuli. Head position/orientation is subject to random perturbations in all directions in daily activities, such as during standing posture, walking, running, going up/down the stairs, bus or metro rides, etc. Powerful stabilizing mechanisms based on complex motor synergies limit head motions in amplitude and frequency during many of these activities (Pozzo et al., 1990; Hirasaki et al., 1999; Carriot et al., 2014; Fino et al., 2020; Wang et al., 2021). One may speculate that the remaining random oscillations might be beneficial by lowering vestibular thresholds with mechanisms similar to SR. If so, the perceptual precision of head motion discrimination and spatial orientation would be enhanced during challenging conditions.

This hypothesis also rests on the notion that vestibular responses are molded on the natural biomechanical behavior of the head. This is demonstrated by the observation that variability and tuning of central vestibular neurons effectively complement the statistics of natural head motion stimuli such as those present during daily activities, thereby achieving temporal decorrelation and optimizing information transmission (Mitchell et al., 2018). Indeed, vestibular discrimination thresholds are affected by neural variability, in addition to neural gain (Carriot et al., 2021). Therefore, one may expect that a given level of random head oscillations, entraining specific populations of central vestibular neurons, enhances vestibular motion discrimination.

A few prior studies added mechanical noise on top of head motion stimuli during motion direction discrimination tasks. In one study (Kabbaligere et al., 2018), wide-spectrum vibrations were applied directly to the mastoid, but they did not significantly change the threshold for yaw rotation at 1 Hz. In another study (Rodriguez and Crane, 2018), vertical whole-body sinusoidal oscillations resulted in horizontal heading-direction thresholds that were worse (higher) than those without the perturbation. However, the applied perturbations involved strong accelerations, presumably out of range to elicit SR effects, as argued by the authors (Rodriguez and Crane, 2018).

Here, differently from these previous studies, we applied small-amplitude, whole-body motion perturbations during the motion discrimination task, and the direction of application of the noise was the same as that of the test stimuli (instead of being orthogonal as in Rodriguez and Crane, 2018). The experiment involved a direction-recognition task, in which the subject reported the perceived direction of the motion (two-alternative forced-choice). First, we determined the individual perceptual thresholds to antero-posterior translations in a baseline condition. Next, we carried out five blocks of trials where we measured again the perceptual thresholds to these translations while simultaneously applying small, stochastic perturbations along the antero-posterior axis, symmetrically distributed around a zero-mean. The power of the perturbations was proportional to the power of the minimum acceleration signal perceived by each participant in the baseline condition (the baseline vestibular threshold). The proportionality coefficient was set at five different values, including a zero-level to verify the consistency of the baseline threshold estimate. We hypothesized that the probability of recognizing a low vestibular directional signal was higher in the presence of noise at some optimal level than in the absence of noise, possibly due to SR effects. If so, the motion discrimination thresholds should be better with noise than without.

EXPERIMENTAL PROCEDURES

Participants

Thirty subjects (21 females; 9 males; 24.6 ± 7.4 years, mean ± SD) participated in the study. They gave written informed consent to procedures approved by the Institutional Review Board of Santa Lucia Foundation (protocol n. CE/PROG0.757), in conformity with the Declaration of Helsinki (World Medical Association, 2013) regarding the use of human participants in research. All participants had normal or corrected-to-normal vision, no history of psychiatric, neurological or vestibular symptoms, dizziness or vertigo, motion-sickness susceptibility, major health problems or medications potentially affecting vestibular function. Sample size was calculated to detect an effect size of 0.8 (Cohen's d, estimated from Keywan et al. (2019) and pilot data with the current setup), by considering paired t-test (R package pwr) with a power of 0.8 and an alpha of 0.05/5 (multiple testing correction), allowing for 25% loss of participants due to various reasons.

Setup

Participants sat in an upright position in a padded racing chair mounted on top of a 6DOF hexapod motion platform (MOOG MB-E-6DOF/12/1000Kg, East Aurora, New York, USA). A 4-point harness held their trunk securely in place. A medium density foam pad under their feet minimized plantar cues about body displacement. Their head was positioned against a rigid headrest in a comfortable posture, centered left to right relative to the earth-vertical and up to down relative to the antero-posterior direction of translation using external landmarks. It was then held in place by means of a tight forehead strap. We monitored 3D position and orientation of both the platform and the participant's head at 200 Hz by means of the Optotrak 3020 system (Northern Digital, Waterloo, Ontario). To this end, four non-coplanar infrared emitting markers were attached to the right side of both the chair and the participant's head. In the latter case, two markers were attached roughly in correspondence of the zygomatic bone, one marker was attached on the tragus, and one marker over the parotid gland. All markers were visible in the initial calibration phase of the experiment. During the test phase, the participants wore active noise-canceling headphones (Bose Noise Cancelling Headphones 700) to mask the acoustic noise from the motion platform. Since the headphones obscured the tragus marker, its virtual position was estimated from a rigid body model of the head constructed from the calibration data. Through the headphones, we also delivered task instructions. To eliminate visual cues during the test phase, the participants kept their eyes closed in the light-tight room. They entered the responses via two buttons of a wireless gamepad. Participants always wore face masks according to the Institution regulations related to COVID-19.

Motion stimuli

Stimuli differed in the baseline trials and in the trials with non-zero perturbations (see Fig. 1 and *Protocol* below). In the former case, the stimuli were pure single cycles of sinusoidal acceleration along the antero-posterior axis (roughly corresponding to the naso-occipital axis), parallel to the earth horizontal plane, in either forward or backward direction:

$$\text{Acceleration } a(t) = A\sin(2\pi ft) \quad (1)$$

$$\text{Speed } v(t) = AT_{norm}[1 - \cos(2\pi ft)] \quad (2)$$

$$\text{Position } p(t) = (AT_{norm})[t - T_{norm}\sin(2\pi ft)] \quad (3)$$

where A is the acceleration amplitude with frequency f = 1 Hz, $T_{norm} = T/(2\pi)$, and T = 1 s is the duration of the motion cycle. In each trial, the value of A was adjusted based on an adaptive staircase (see *Procedure*). The time profile of these stimuli does not involve position, velocity, or acceleration discontinuities, it has been consistently used in previous studies of self-motion perception (e.g., Bermúdez Rey et al., 2016; Bremova et al., 2016; Kobel et al., 2021; Valko et al.,

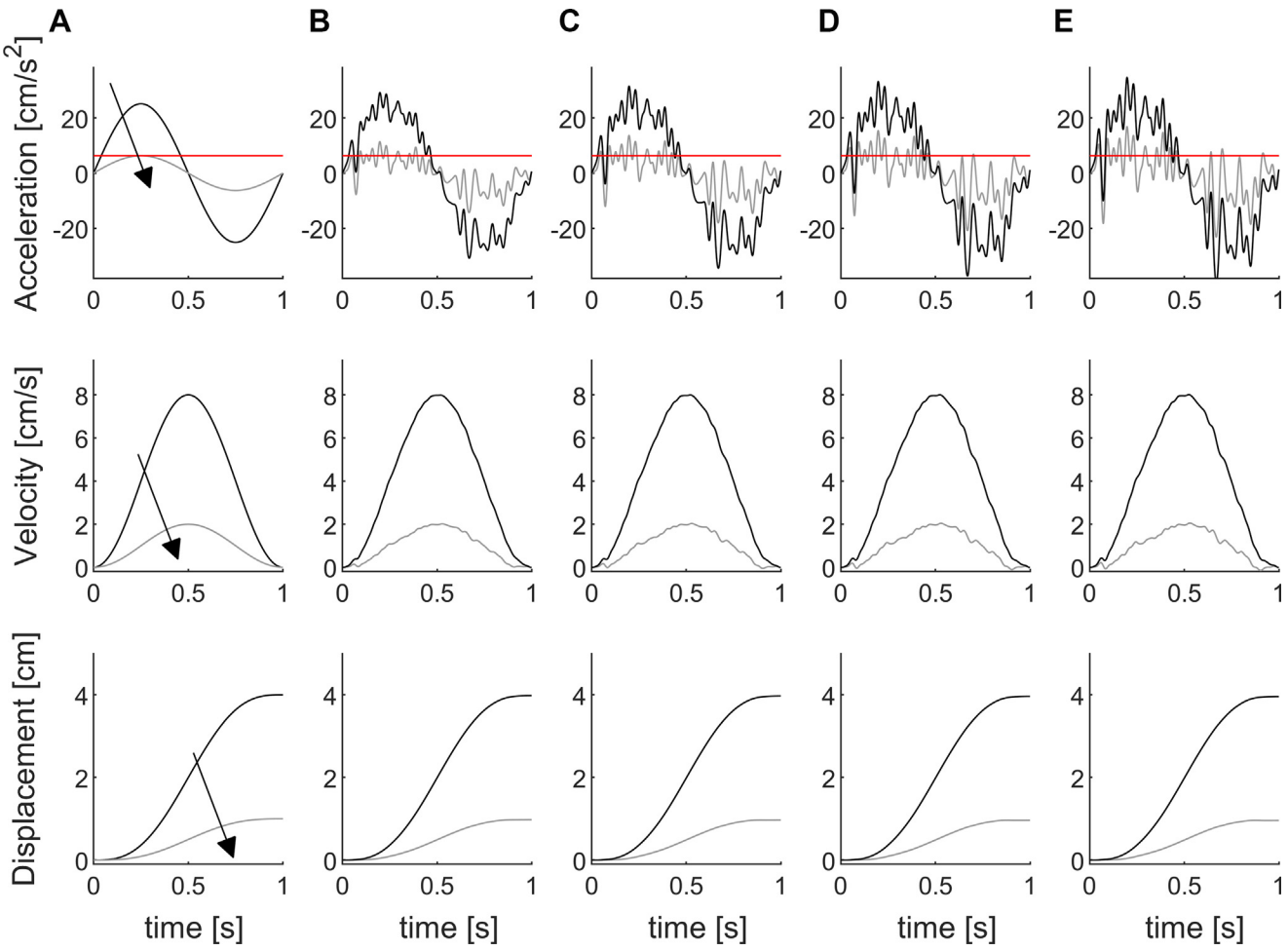

Fig. 1. Motion stimuli consisting of a single cycle of 1 Hz sinusoidal accelerations along the antero-posterior direction (top row), the corresponding velocities (middle row) and displacements (bottom row). A: Black and gray correspond to unperturbed stimuli with peak velocities of 8 cm/s and 2 cm/s, respectively. The arrow indicates the direction of changes following a theoretical adaptive staircase. B: Perturbed stimuli with peak velocities of 8 and 2 cm/s in the noise condition with intensity proportional to a vestibular threshold of 2 cm/s and $k = 0.5$. C, D and E: The same of panel B but $k = 1$, 1.5 and 2, respectively. In the top row, the red line denotes the peak value of acceleration corresponding to a vestibular threshold of 2 cm/s.

2012), and resembles the time profile of head motions during natural behaviors such as walking (Hirasaki et al., 1999).

Motion thresholds correspond to the minimum stimulus amplitude reliably perceived. In the following, we report vestibular thresholds using the peak velocity of the smallest stimulus that was reliably perceived by each participant in a given condition. Because acceleration, speed, and position are all proportional between each other in Eqs. (1–3), the results are unchanged if presented as displacement thresholds, velocity thresholds, or acceleration thresholds (Chaudhuri et al., 2013). However, for the sake of comparison with other studies, we also report acceleration thresholds (peak of stimulus acceleration at threshold).

In the trials with perturbations, noise of different intensity was superimposed onto the same sinusoidal test stimuli used in the baseline trials (Fig. 1). Noise consisted of random fluctuations of acceleration along the antero-posterior axis, mimicking head and body oscillations that could be experienced during daily life (Fino et al., 2020). The direction of application of the noise was the same as that of the test stimuli. Noise power was proportional to the power of the acceleration stimulus corresponding to the individual threshold determined for each participant during the baseline condition. Specifically, we generated offline (at 1 kHz) white noise $\varepsilon(t)$, 1-s duration, which was band-pass filtered within 1.8 Hz – 30 Hz (infinite impulse response filter of order 20, Matlab function *bandpassiir*), reduced to zero-mean by subtracting the mean value, and normalized to unit-power. The frequency range of the applied noise (1.8 Hz – 30 Hz) was chosen to mimic that of previous studies showing SR-effects on motion discrimination with stochastic galvanic vestibular stimulation (Galvan-Garza et al., 2018; Putman et al., 2021).

This unit-power noise was scaled in amplitude as a function of the variance δ^2 of the acceleration at the individual baseline threshold:

$$\varepsilon^*(t) = \varepsilon(t)\sqrt{k\delta^2} \quad (4)$$

The proportionality constant k was 0, 0.5, 1, 1.5, or 2 in different blocks of trials, presented in randomized order. The overall acceleration stimuli applied in the trials with noise were:

$$a(t) = Asin(2\pi ft) + \varepsilon^*(t) \quad (5)$$

Notice that the value of A changed from trial to trial according to the adaptive staircase in the same manner in the trials with and without noise, but the added noise $\varepsilon^*(t)$ was the same in all trials of a given block. While the time profile of the noise was identical for all participants, the noise amplitudes were specific to each participant, being related to the individual baseline thresholds according to Eq. (4).

By design, the noise $\varepsilon^*(t)$ was symmetrically distributed around a zero-mean not to provide any directional cue independently of the potential interaction with the test stimuli.

All position profiles were programmed in LabVIEW 2020 (National Instruments, Austin, Texas, USA) with custom-written software, and input to the MOOG controller at 1 kHz.

Pilot experiments showed that the addition of noise perturbations on top of the motion stimuli was well tolerated and even went unnoticed by the participants.

Rationale for noise levels

Some previous GVS studies have employed fixed levels of noise across all participants, while other studies have used noise levels specific to each subject, and it is unknown which approach is more valid for GVS applications (e.g., Goel et al., 2015; Mulavara et al., 2015; Galvan-Garza et al., 2018; Keywan et al., 2018, 2020a; Voros et al., 2021). Here, we chose to set noise amplitudes proportional to individual thresholds based on the following considerations. In contrast with GVS, the mechanical noise we used does not bypass the biomechanics of the test motion stimuli, since noise and stimuli are physically superimposed. Therefore, it is critical that the noise amplitude is calibrated on the individual motion threshold, else it might turn out too strong or too weak to keep the overall input (signal plus noise) close to the baseline threshold. From the literature, we know that vestibular thresholds can vary widely across subjects, even up to two orders of magnitude (e.g., Guedry, 1974; Bermúdez Rey et al., 2016; Diaz-Artiles and Karmali, 2021). We also observed substantial inter-subject variability of the thresholds in our pilot experiments. Accordingly, we chose to adjust noise amplitudes as a function of the individual baseline thresholds.

As for the choice of the different values of proportionality constant k in Eq. (4), the rationale was the following. The condition with $k = 0$ was identical to the baseline, and represented an experimental control to verify the consistency of the baseline threshold estimate, as well as to check for a possible ordering effect. While the baseline was always done first, the condition with $k = 0$ was randomly intermingled with the conditions with $k = 0.5$, 1, 1.5, or 2 in different blocks of trials. The conditions with $k = 0.5$, 1, 1.5, or 2 were aimed at generating noise with root-mean-square (RMS) acceleration identical to the RMS of the test acceleration stimulus at baseline threshold multiplied by $\sqrt{k}$. Thus, RMS_{acc} of the noise was equal to:

$$RMS_{acc} = \frac{\pi \sigma_{base} \sqrt{k}}{\sqrt{2}} \quad (6)$$

where σ_{base} was the velocity threshold in the baseline condition.

Predictions based on threshold crossings

By looking at Fig. 1, one can appreciate the potential implications of applying different levels of noise whose amplitude is tailored specifically to the individual baseline threshold. One may consider two different hypotheses to account for potential performance improvements (reduction of motion discrimination threshold) as a function of noise amplitude.

According to one hypothesis, the discrimination performance depends on a simple superposition of noise and stimulus. As the amplitude of noise increases (from panel A to panel E in Fig. 1), the peak acceleration of the overall input (stimulus plus noise) increases proportionally to noise. Therefore, if the improvement in threshold depends on a net increase of peak acceleration, one would expect that the threshold improvement should vary monotonically with noise amplitude, i.e., the higher the noise the greater the improvement.

By contrast, according to non-linear behaviour such as due to SR-like substrates, improvement varies non-monotonically with noise amplitude, being maximum at some optimal level and decreasing for higher levels of noise. The lower amplitude perturbations (panels B-D, corresponding to $k = 0.5$, 1, 1.5) can facilitate threshold crossing (red line in Fig. 1) by the combination of stimulus plus noise, but only during the first acceleration phase (0–0.5 s epoch). In this manner, the resulting vestibular signals for motion discrimination could be boosted relative to the condition without noise. When the amplitude of the noise is higher (panel E, corresponding to $k = 2$), however, noisy oscillations can cross the threshold during both the first and the second acceleration phase (in the opposite direction relative to the first phase, 0.5–1 s epoch), swamping the stimulus waveform. Therefore, although also the higher noise allows exceeding the baseline threshold, the vestibular system may now be unable to distinguish between signal and noise. This hypothesis then predicts that the new discrimination threshold would be improved relative to the baseline in the presence of lower amplitude noisy perturbations ($k = 0.5$, 1, 1.5), but not with higher amplitude noise ($k = 2$).

Procedure

To determine the perceptual thresholds, we used a 3Down-1Up adaptive staircase (Leek, 2001; Grabherr et al., 2008; Karmali et al., 2016). Initial peak speed of the unperturbed motion stimulus was 8 cm/s, above the presumptive threshold in each participant (Diaz-Artiles and Karmali, 2021). The peak acceleration was

25.13 cm/s^2, and the maximum displacement was 4 cm. Until the first mistake, the stimulus was halved after three correct responses at each level. From this point onward, the size of the change in stimulus amplitude was determined using parameter estimation by sequential testing (PEST) rules (Taylor and Creelman, 1967). The minimum step size was 0.38 dB (i.e., 1.25 $\log_{10}2$), and the maximum step size was 6.02 dB (i.e., 20 $\log_{10}2$). Motion direction (forward or backward) was randomized in each trial. The randomization procedure ensured that there was the same number of forward and backward motions every 20 trials. After each stimulus, participants indicated the perceived direction of motion (forward or backward, two-alternative forced-choice direction recognition task). When they were unsure of the direction, they were asked to make their best guess. No feedback was provided as to the correctness of the responses. In each trial starting from the 25th, we iteratively fitted a running psychometric curve with a generalized linear model (GLM) and we computed the coefficient of variation of the σ parameter (see *Data analysis*). The block of trials was terminated after 100 trials or when CV of σ reached 0.2, whichever occurred first.

Protocol

Participants received detailed instructions about the procedure prior to the experiment. However, neither the possible presence of noise perturbations nor the purpose of the experiment was disclosed. All participants performed six blocks of trials, split in two sessions on two separate days (separated by about 8 days) to avoid fatigue, with three blocks of trials in each session. Before each session, head position and orientation were recorded over 5 s during a calibration phase and the average values used as a reference for the following trials. Calibration was repeated during the session if necessary (e.g., when the participant stepped down the chair to rest). Next, six suprathreshold (8 cm/s speed, 1 Hz), practice trials without noise were administered to make sure that the participant was comfortable with the task. On day 1, the first block always involved the determination of the baseline threshold using motion stimuli without noise perturbations (Eq. (1)). This baseline threshold was used to compute the individual noise level for the trials with added perturbations. The next five blocks of trials involved the five noise levels (k = 0, 0.5, 1, 1.5, 2 in Eq. (4)) in randomized order, counterbalanced across participants. The condition with k = 0 was the same as the baseline, and it was randomly interspersed with the others with non-zero noise. Each block of trials lasted about 13 min, with about 10-min rest breaks between blocks. No participants -interviewed after the end of the experiment on day 2- reported having being aware of the presence of noise perturbations.

The time sequence of events during each trial was the following (Fig. 2). The participant pressed a button when ready for the trial after hearing a pre-recorded voice message. Before starting the motion stimuli, we checked that the head had not moved appreciably relative to the reference of the calibration phase. To this end, we acquired 3D head position and orientation over 500 ms, and computed the mean shift relative to the reference. The shift in position was calculated as the 3D distance of the tragus from its reference position. The

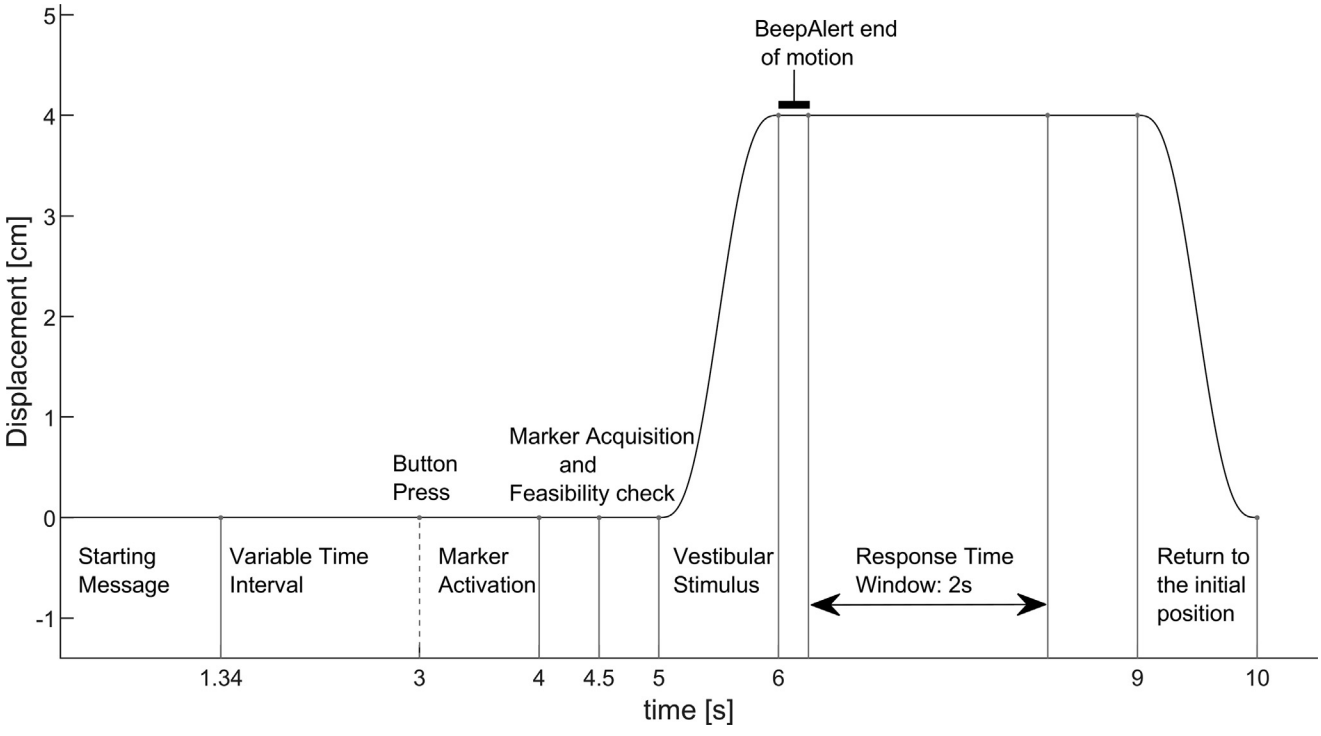

Fig. 2. Time sequence of events during each trial. Displacement of the chair relative to the initial position is plotted as a function of time.

tilt was calculated separately for roll, pitch and yaw from the reference angles. If the shift was less than ≈2 cm for position and ≈5° for tilt, platform motion could start. Else, the participant's head was repositioned within the described tolerance window, and the trial started again with the voice message. The time interval between the button press and the motion start was 2 s. Two consecutive sounds (each with frequency of 500 Hz, duration of 125 ms) signaled the end of platform motion. Within the next 2 s epoch, participants had to indicate the perceived motion direction by pressing the fore or aft button of the hand-held gamepad, depending on whether they perceived a forward or backward motion, respectively. If they responded too early or too late, a different sound (frequency 250 Hz, duration 800 ms) signaled the error, and the response was considered incorrect. They were maintained in the final position for 3 s, then they were moved back to the initial position with the same kinematics of the last stimulus but in the opposite direction. Thus, the time interval between the start of platform motion and the return to the initial position was 5 s. The minimum inter-trial interval was 3.34 s to mitigate motion after-effects (Crane, 2012). During the platform motion, a running average of 3D head position and orientation over 50-ms consecutive intervals was computed on-line. If the head shifted by > 0.5 cm or rotated by > 2.5° (in either roll, pitch or yaw) relative to the chair (and platform) over any 50-ms interval, the trial was discarded and repeated.

Data analysis

Data analyses were performed with Matlab 2021b (The MathWorks, MA, USA). We fit a Gaussian cumulative distribution psychometric function with standard deviation (σ) and mean (μ) to the responses with a maximum likelihood estimate via a GLM and a probit link function (Merfeld, 2011). The threshold parameter represents the "one-sigma" vestibular threshold and corresponds to (1) the standard deviation of the underlying distribution function and (2) the stimulus level that would be expected to yield 84.1% correct performance in the absence of bias (Merfeld, 2011). Each data set was also fit using a bias-reduced generalized linear model (BRGLM, Matlab function *brglmfit*) to correct potential misestimates of σ when fitting serially dependent data (Chaudhuri and Merfeld, 2013; Karmali et al., 2016). Moreover, we fit the psychometric function using a lapse-identification algorithm (LIA, deltadeviance method, Clark and Merfeld, 2021) based on a standard delete-one jackknife procedure to identify probable spurious datapoints of the staircase (Tukey, 1958). Lapses are errors made by participants independently of the test stimuli, such as those due to inattention, fatigue etc.

Characterization of mechanical stimuli

We carried out separate tests to verify that the mechanical perturbations were equivalent when applied during forward and backward translations, so as not to provide any directional cue independently of the potential interaction with subthreshold test stimuli. To this end, 3D linear accelerations were recorded at 200 Hz with an MPU-6050 sensor (TDK InvenSense, San Jose, California, USA, operated at full scale range of ±2 g) attached to the base of the MOOG platform under the chair, while position of the markers on the chair was recorded by the Optotrak at the same rate. Data were acquired during conditions replicating those experienced by our participants when they were close to a typical value of perceptual threshold (see *Results*). Thus, we applied 1-Hz single-cycle sinusoidal accelerations with peak velocity of 2 cm/s in either forward or backward direction, and noise intensity proportional to the vestibular threshold of 2 cm/s and $k = 1$ (Eq. (4)). In each trial, we recorded a 2 s time epoch extending 0.5 s before and after the motion trajectory. We performed 100 trials for each motion direction (forward and backward). Data analysis followed that of Chaudhuri et al. (2013) for both positions and accelerations. To minimize potential biases and drifts, the mean value for the first and the last 0.2 s was subtracted from the data of each trial. Then, we computed the average for each of the three orthogonal linear acceleration (position) components at each instant in time over all 100 trials for each direction. Using the three average components of acceleration (position), we computed the module of acceleration (displacement) in forward and backward direction at each instant in time. We found that the module of acceleration and position were not significantly different between forward and backward direction. Thus, the mean difference between the module of acceleration in forward and backward direction was 0.06 cm/s^2 [95%CI −0.04 0.17], while the mean difference between the module of displacement in forward and backward direction was 0.0002 cm [95%CI −0.0001 0.0004].

We also used the results of these tests to verify that the actual position profiles generated by our MOOG platform matched the programmed profiles, since mechanical dynamics might result in a mismatch (Karmali et al., 2014). We found that the mean difference between the module of position measured by the Optotrak and the module of the position signal input to the MOOG was −0.0010 cm [95%CI −0.0853 0.0833] and −0.0008 cm [95%CI −0.0853 0.0836] in forward and backward direction, respectively.

Statistics

Statistical analyses were performed in R (4.0.2). Individual threshold values were first log transformed, because the results with GLM and BRGLM demonstrated a lognormal distribution in all participants, consistent with previous reports (Grabherr et al., 2008). We used the Shapiro–Wilk test to verify the normality of distribution of data. We also verified whether there were outlier participants by applying the R function identify_outliers (rstatix package) to the individual threshold values of the baseline block. Although our study was not designed to explore sex differences nor powered for this purpose (due to the imbalance between female and male participants), we performed unpaired t-tests on each experimental condition (baseline and $k = 0$, 0.5, 1, 1.5, and

2) to test for possible effects of sex on the vestibular thresholds of the present sample of participants.

To test for effects of noise on motion discrimination, log-transformed thresholds were subjected to repeated-measures analysis of variance (RM-ANOVA) with noise intensity as the within-subjects factor (six levels, baseline and k = 0, 0.5, 1, 1.5, and 2). Effect size was computed as partial eta square η_p^2. Additionally, preplanned comparisons testing performance for each of the five noise intensities (k = 0, 0.5, 1, 1.5, or 2) against the baseline were performed and corrected for multiple comparisons by means of the Bonferroni method (using the R function pairwise_t_test). The baseline represented the reference condition because it was performed prior to any addition of noise, and therefore it could not be affected by the exposure to noise in a prior block. The control condition, being randomly intermingled with non-zero noise conditions, was potentially susceptible to after-effects from prior exposure to noise. Therefore, as explained in a previous section, the zero-noise (k = 0) control condition served the purpose of verifying the consistency of the baseline threshold estimate as well as possible ordering effects.

When the log-transformed thresholds were not normally distributed (with the lapse-identification LIA), we used non-parametric statistics to test the effects of noise (Friedman test). Post-hoc corrections for multiple comparisons were performed with Wilcoxon test (R function wilcox_test).

Population responses were also analysed by means of a Generalized Linear Mixed Model (GLMM) that separately accounts for the random effects due to inter-subject variability and the fixed effects due to the experimental variables (Moscatelli et al., 2012). To this end, we fitted the data of the different participants and experimental conditions with the following GLMM:

$$\Phi^{-1}\left[P(Y_{ij}=1|\mathbf{u}_i)\right] = \alpha_0 + u_{0i} + (\beta_1 + u_{1i})S_{ij} + \sum_{n=1}^{5}((\alpha_n k_n^{ij}) + \beta_n S_{ij} k_n^{ij}) \quad (7)$$

The left side of the equation is the probability that participant i in trial j reported that the platform motion was in the forward direction, with Φ^{-1} being the probit transform of this probability (i.e., the inverse of the cumulative Gaussian function). The right side of the equation is a linear combination of the fixed (α and β) and random (u) effects predictors. Specifically, S_{ij} is the amplitude of the stimulus and k_n^{ij} (with n = 1:5) are the categorical predictors coding for the perturbed conditions (with noise level of k = 0, 0.5, 1, 1.5, 2). The first unperturbed condition represented the baseline in the model. The fixed effects estimated the effect of the experimental variables common to all participants. The fixed effects α_0, and β_0 correspond to the intercept and the slope of the baseline condition. The inverse of the slope represents the threshold (σ): the higher the slope, the lower the threshold. The slope of the condition with a given level of noise (k(n)) is equal to the sum of β_0 and β_n. If the threshold of a condition with noise (σ_n) was not significantly different from the baseline (σ_{base}), then β_n would not be significantly different from zero (the null hypothesis). The fixed-effect parameters α_n provided an adjustment to the intercept in each noise condition. The random-effect parameters u_{0i} and u_{1i} estimated the heterogeneity between participants. Alpha was set to 0.05 for all statistics.

Stochastic resonance curve fitting

In order to visually assess if SR-like effects were recognizable in our experimental data, the plot of population threshold values versus noise levels was best-fit (least-squares method) with a quartic equation previously developed to describe general SR phenomena (Rouvas-Nicolis and Nicolis, 2007):

$$A = \varepsilon\frac{\lambda}{q^2}\frac{r(q^2)}{\sqrt{r(q^2)^2 + \omega_0^2/4}} \quad (8)$$

where A is the amplitude of the response, q^2 is the variance of the noise strength (i.e., $k\delta^2$) and

$$r(q^2) = \frac{1}{\sqrt{2\pi}}\lambda e^{-\frac{\lambda^2}{2q^2}} \quad (9)$$

The additional system parameters include the amplitude ϵ of weak periodic forcing, the frequency ω_0 of weak periodic forcing, and the quartic potential parameter λ (related to depth and spread of the potential wells). Notice that the curve fit only served as a visualization aid for qualitative judgment of SR-like exhibition, and not as a formal mathematical representation of vestibular perceptual SR (Galvan-Garza et al., 2018).

Unbiased analysis of performance improvement under optimal noise levels

To determine unbiased values of the optimal noise level and of the associated performance improvement for each subject, we used a bootstrap approach on independent data sets as proposed by van der Groen and Wenderoth (2016) for a similar purpose. To this end, we randomly split all trials in half for each subject (n = 30) and each experimental condition (baseline, k = 0, 0.5, 1, 1.5, 2). One-half of the trials (*discovery data set*) were used to define the optimal noise level (i.e., the noise value that causes the best discrimination performance, i.e., the lowest threshold across all noise conditions k = 0.5, 1, 1.5, 2). The other half of the trials (*test data set*) were used to determine the performance improvement observed for the optimal noise level "discovered" from the first data set. Performance improvement was computed relative to either the baseline performance ($\sigma_{OptimalNoise}/\sigma_{base}$) or the zero-noise performance ($\sigma_{OptimalNoise}/\sigma_{k=0}$). The procedure was repeated 1000 times for each participant to obtain the average optimal noise level and the average performance improvement associated with the optimal noise level.

RESULTS

Motion stimuli and perturbations

Each participant underwent six experimental conditions with two blocks of trials involving unperturbed stimuli (the baseline and the control with $k = 0$) and four blocks of trials involving perturbed motion stimuli ($k = 0.5, 1, 1.5, 2$). In each block, participants performed 77.5 ± 11.6 valid trials (mean ± SD, n = 180 [30 participants × 6 blocks]) before reaching the preset target. Due to inattention or head movements outside the tolerance window (see *Methods*), there were also 4.03 ± 6.2 (mean ± SD, n = 180) invalid trials that were discarded and repeated during the block. The number of both valid and invalid trials did not depend significantly on the 6 experimental conditions (P = 0.5 and 0.23 respectively, Friedman test).

While the sinusoidal motion stimuli were the same for all participants in all trials (both unperturbed and perturbed), the noise intensities in the perturbed trials were specific to each participant, depending on the individual baseline thresholds (see *Methods*). To document the variability of noise amplitude across subjects, Fig. 3 shows the stimuli without noise (black) and with noise proportional to the minimum (red), maximum (blue) and median (green) vestibular thresholds (over all participants, n = 30).

The mean amplitude of the sinusoidal test stimuli (i.e., the platform displacement) in correspondence of the baseline threshold (see below) was 1.14 cm ± 0.34 cm (mean ± SD, n = 30 participants). By comparison, the mean amplitude (maximum – minimum) of displacement due to the noise perturbations was 0.027 cm ± 0.008 cm (mean ± SD, n = 30), 0.038 cm ± 0.011 cm, 0.047 cm ± 0.014 cm, 0.054 cm ± 0.016 cm for noise level $k = 0.5, 1, 1.5, 2$, respectively. Thus, the displacement due to noise was less than 5% of the smallest displacements that were reliably perceived by the participants.

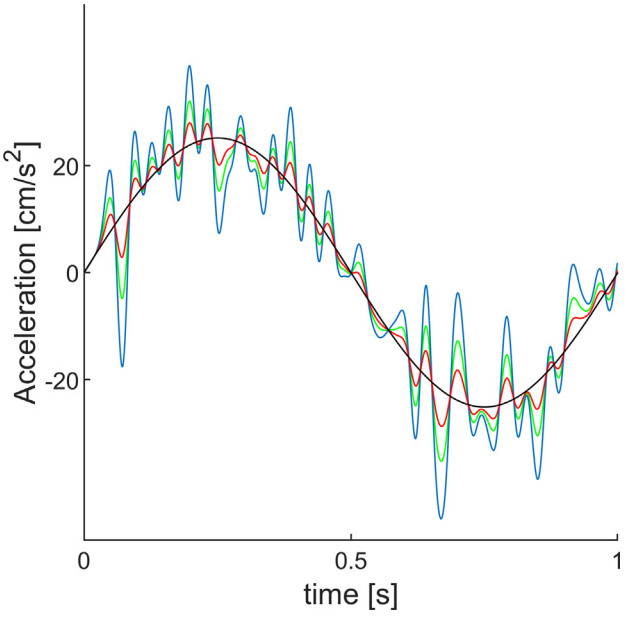

Fig. 3. Stimuli at peak velocity of 8 cm/s without noise (baseline and $k = 0$, black) and with noise ($k = 1$) proportional to the minimum (red), maximum (blue) and median (green) values of vestibular thresholds computed over all participants.

The geometric means of root-mean-square (RMS) acceleration of the noise perturbation was 3.44 cm/s^2 (95% CI [3.08 3.85], n = 30), 4.87 cm/s^2 (95% CI [4.35 5.44], n = 30), 5.96 cm/s^2 (95% CI [5.33 6.66], n = 30), and 6.88 cm/s^2 (95% CI [6.16 7.69], n = 30) for noise level $k = 0.5, 1, 1.5, 2$, respectively. Because of the way noise was derived (Eq. (4)), its RMS acceleration was identical to the RMS of the test acceleration stimulus at baseline threshold multiplied by $\sqrt{k}$ (Eq. (6)).

Head stability

At the start of the trial, the shift of the head in 3D relative to the calibration reference was 0.3 cm ± 0.4 cm (mean ± SD, n = 180), and −0.51° ± 1.36°, 0.89° ± 2.76, 0.57° ± 1.48 (mean ± SD, n = 180) in roll, pitch and yaw, respectively. During platform motion, the absolute value of the shift of the head in 3D relative to the platform was 0.07 cm ± 0.02 (mean ± SD, n = 180), and 0.58° ± 0.19°, 0.17° ± 0.06°, 0.87° ± 0.24° (mean ± SD, n = 180) in roll, pitch and yaw, respectively. Neither the head shift at trial start nor that during platform motion depended significantly on the experimental condition (all P > 0.09, Friedman test).

Thresholds

We found that the log-transformed thresholds computed with GLM were normally distributed for all six experimental conditions (baseline and $k = 0$, 0.5, 1, 1.5, and 2, all P-values > 0.178, Shapiro–Wilk test). The thresholds of each participant and each condition are plotted in Fig. 4. There was considerable inter-subject variability, and there were no outlier participants for the baseline condition. Vestibular thresholds for the six experimental conditions did not depend significantly on sex (unpaired t-test, all P > 0.26), consistent with previous results (Bermúdez Rey et al., 2016; Wagner et al., 2022).

Importantly, the threshold in 26/30 participants (87%) was lower with at least one noise intensity than the corresponding values in both unperturbed conditions (the baseline and the control with $k = 0$), indicating that low amplitude noise added to vestibular stimulation can improve the perception of motion direction. In 20 of these 26 participants (77%), the threshold at the highest level of applied noise ($k = 2$) was worse than the threshold at a lower level of noise ($k = 0.5$, 1 or 1.5).

A RM-ANOVA over the responses of all 30 participants showed that the threshold was significantly different as a function of the six experimental conditions ($F(5,145) = 4.17$, $P = 0.001$, $\eta_p^2 = 0.130$). Post-hoc tests showed that neither the threshold for the control condition nor that for the highest level of noise ($k = 2$) differed significantly from the baseline threshold (uncorrected P = 0.081 and P = 0.013, respectively).

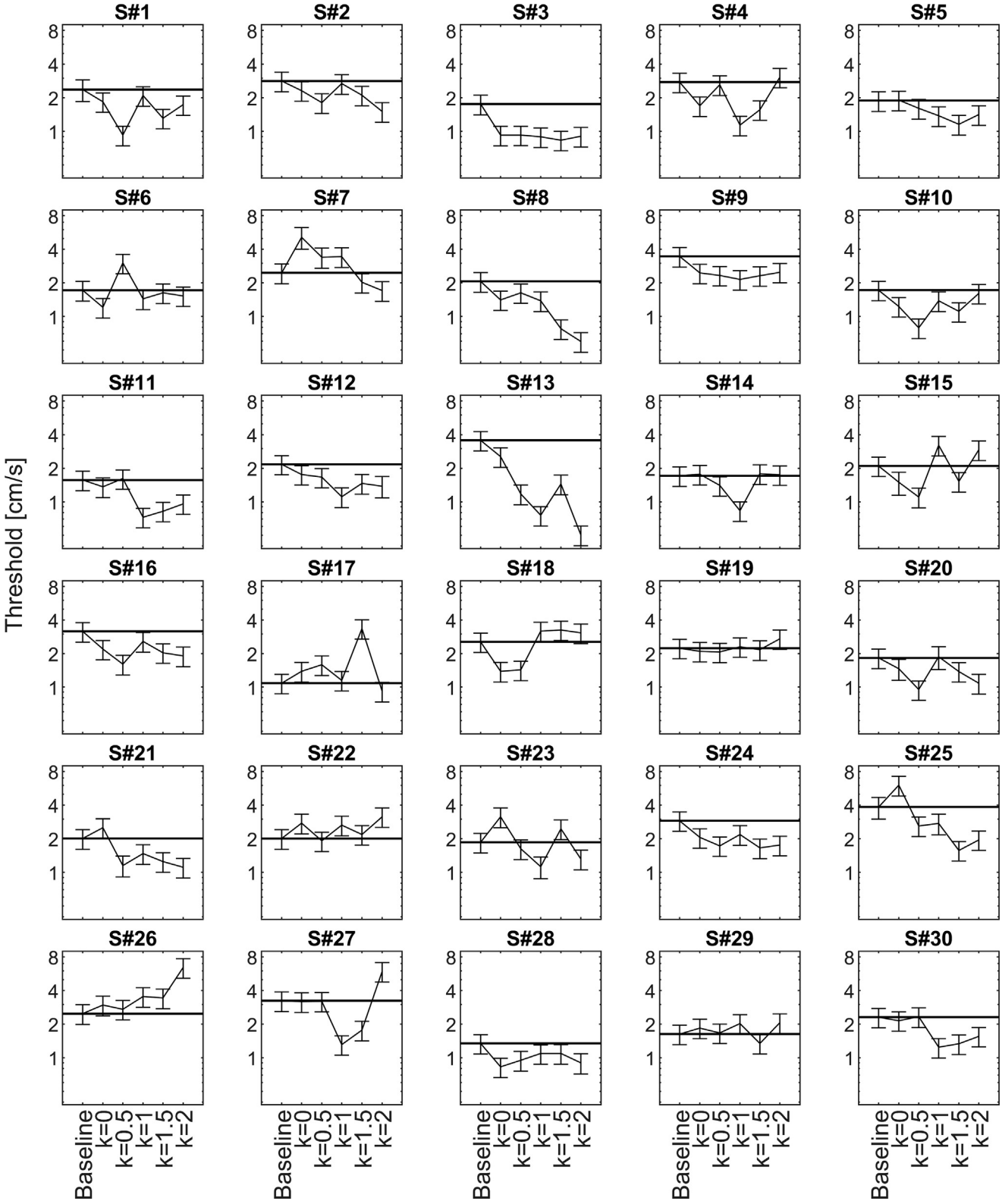

Fig. 4. Motion discrimination thresholds of each participant as a function of experimental conditions (error bars indicate the standard deviation of the threshold estimate). The horizontal lines indicate the threshold values in the baseline condition. Threshold values are plotted in logarithmic scale (y-axis).

By contrast, the thresholds with noise levels k = 0.5, 1 and 1.5 were significantly lower than the baseline (all $P < 0.009$ after Bonferroni correction, Fig. 5). Table 1 reports velocity thresholds while Table 2 reports acceleration thresholds. As a mere visualization aid to compare the results with SR-like behavior, the

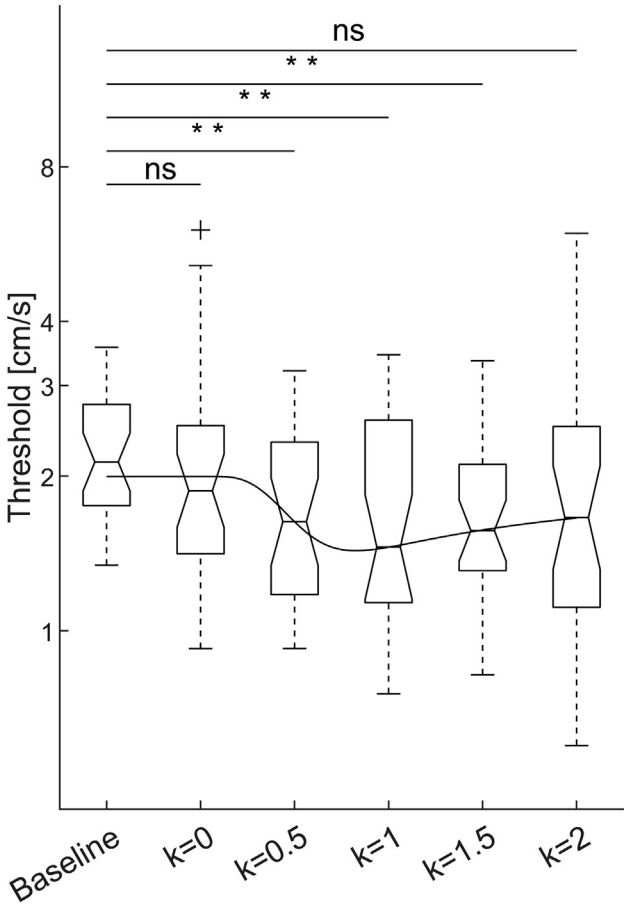

Fig. 5. Motion discrimination thresholds at population level. The thresholds with noise intensity k = 0.5, 1 and 1.5 were significantly lower than the baseline threshold (**, P < 0.01). The threshold for the control condition (k = 0) and that for the highest level of noise (k = 2) were not significantly different from the baseline threshold. In the box-and-whisker plots, the box corresponds to the median and the 25th and 75th quartiles, and the whiskers show the 5th and 95th percentile. '+' marker symbol denotes an outlier. Overlaid line is the best fit of the population threshold data with SR-like equation. Threshold values are plotted in logarithmic scale (y-axis).

continuous line of Fig. 5 depicts the best fit of the population threshold data with an equation previously developed to describe general SR phenomena (Eq. (8) in Methods).

The zero-noise control condition (k = 0) was randomly intermingled with the non-zero noise conditions (k = 0.5, 1, 1.5, 2) in different blocks of trials to verify the consistency of the baseline threshold estimate, as well as to check for a possible order effect. Consistency was shown by the lack of a statistically significant difference between the control and the baseline threshold (see above). Lack of statistically significant order effects was shown by a RM-ANOVA with block order as within-subjects factor (five levels, k = 0, 0.5, 1, 1.5, and 2) over the thresholds of all 30 participants ($F(4,116) = 1.72$, $P = 0.150$, $\eta_p^2 = 0.05$).

Thresholds were also computed with the Generalized Linear Mixed Model (GLMM) that separately accounts for the random effects due to inter-subject variability and the fixed effects due to the experimental variables (Eq. (7)). The GLMM confirmed the previous results by showing that the slope of the responses (the inverse of the slope corresponds to the threshold, see *Methods*) was significantly higher (implying a lower threshold) for the conditions with noise levels k = 0.5, 1 and 1.5 than the slope for the baseline ($P < 0.001$). By contrast, the slopes of the responses for the control condition (k = 0) and for the highest level of noise (k = 2) were not significantly different from the slope of the baseline (all $P > 0.09$).

We obtained very similar results by calculating the thresholds with the bias-reduced generalized linear (BRGLM) model or with the lapse-identification algorithm (LIA, Table 1). In both cases, the threshold was significantly different as a function of noise (with BRGLM, $F(5,145) = 4.281$, $P = 0.001$, $\eta_p^2 = 0.129$; with LIA, Friedman test $\chi^2(5) = 13.1$, n = 30, $P = 0.023$, $\eta_p^2 = 0.087$).

Performance improvement with optimal noise levels

Consistent with several previous studies (e.g., Collins et al., 1996b; Martínez et al., 2007; Van der Groen and Wenderoth, 2016), we found substantial inter-individual variability in the optimal noise level, that is, the noise level leading to the best performance (see Fig. 4). Moreover, as we remarked before, the noise intensities in the perturbed trials differed across participants, depending on the individual baseline thresholds. Therefore, we compared the lowest thresholds obtained in each individual irrespective of the noise level (k = 0.5, 1, 1.5 or 2) with the thresholds obtained in the unperturbed conditions (baseline and k = 0). On average, the optimal individual noise reduced thresholds by 42% ± 20% (mean ± SD, n = 30) relative to the baseline thresholds, and by 34% ± 24% (mean ± SD, n = 30) relative to the control (k = 0) condition. We found a significant positive correla-

Table 1. Vestibular thresholds (peak velocity of the smallest stimulus that was reliably recognized) computed with different methods (see text). For GLM, BRGLM and GLMM, the values correspond to the geometric means. For LIA, the values correspond to the medians, since the data were not normally distributed. 95% confidence intervals are between brackets

Experimental Condition	Motion thresholds (cm/s)			
	GLM	BRGLM	LIA	GLMM
Baseline	2.191 [1.961 2.449]	2.302 [2.057 2.575]	1.945 [1.694 2.236]	2.183 [1.885 2.526]
k = 0.0	1.958 [1.662 2.308]	2.044 [1.736 2.440]	1.841 [1.564 2.169]	2.053 [1.750 2.387]
k = 0.5	1.654 [1.426 1.919]	1.732 [1.493 2.009]	1.609 [1.315 1.969]	1.776 [1.572 2.016]
k = 1.0	1.652 [1.386 1.969]	1.725 [1.448 2.056]	1.456 [1.214 1.755]	1.851 [1.590 2.094]
k = 1.5	1.616 [1.399 1.867]	1.695 [1.468 1.957]	1.483 [1.274 1.725]	1.730 [1.557 1.939]
k = 2.0	1.682 [1.354 2.089]	1.759 [1.418 2.182]	1.662 [1.211 2.081]	2.026 [1.757 2.283]

Table 2. Vestibular thresholds computed as the peak of stimulus acceleration at threshold; geometric means and 95% confidence intervals between brackets

Experimental Condition	Motion thresholds (cm/s^2)
	GLM
Baseline	6.884 [6.160–7.694]
k = 0.0	6.152 [5.220–7.251]
k = 0.5	5.197 [4.478–6.030]
k = 1.0	5.189 [4.353–6.186]
k = 1.5	5.076 [4.394–5.866]
k = 2.0	5.284 [4.255–6.563]

tion between the threshold values in the unperturbed conditions and the maximum noise-induced improvement (r(30) = 0.37, P = 0.044, and r(30) = 0.55, P = 0.0018, for baseline and control, respectively). Thus, participants with higher thresholds in the unperturbed conditions benefitted more from added noise than participants with lower unperturbed thresholds. On the other hand, participants with higher unperturbed thresholds did not require a significantly greater level of noise to reach optimal performance as compared with participants with lower unperturbed thresholds (r(30) = −0.01, P = 0.96).

We also assessed the performance improvement with optimal noise on independent data sets (to avoid statistical "double dipping"). In this case, we determined independently the optimal noise level and the associated discrimination performance improvement with a bootstrap approach for each participant (see *Methods*). The thresholds estimated with this method were similar to those reported above using standard methods (see Table 1): the mean threshold was 2.33 cm/s [95%CI 2.15 2.54], 2.23 cm/s [95%CI 1.97 2.52] and 1.63 cm/s [95%CI 1.44 1.84] for the baseline, k = 0 and optimal noise level, respectively. The performance improvement relative to the baseline performance ($\sigma_{OptimalNoise}/\sigma_{base}$) was normally distributed (P = 0.44, Shapiro–Wilk test). The improvement with the optimal individual noise was statistically significant (paired t-test, t(29) = 5.6893, P = 0.000003, η_p^2 = 0.527). On average, the optimal individual noise reduced thresholds by 23% relative to the baseline.

Similar results were obtained by computing the best performance improvement relative to the performance in the control (k = 0) condition ($\sigma_{OptimalNoise}/\sigma_{k=0}$). Also in this case, the distribution of performance improvement was normally distributed (P = 0.43, Shapiro–Wilk test). The improvement with the optimal individual noise was statistically significant (paired t-test, t(29) = 3.0365, P = 0.005,η_p^2 = 0.241). On average, the optimal individual noise reduced thresholds by 17% relative to the control.

Relationship between threshold and noise amplitude across subjects

One may consider two competing hypotheses to account for performance improvements as a function of noise amplitude. According to non-linear SR-like substrates, improvement varies non-monotonically with noise amplitude, being maximum at some optimal level and decreasing for higher levels of noise. By contrast, according to simple superposition of noise and stimulus, improvement varies monotonically with noise amplitude, the higher the noise the greater the improvement. We already remarked that the threshold varied non-monotonically with noise at the population level (Fig. 5), and at the level of most individual participants (Fig. 4). In particular, the threshold at the nominal noise level of k = 2 did not differ significantly from the baseline at the population level, and it was worse than the threshold at a lower level of noise (k = 0.5, 1 or 1.5) in most subjects.

However, it could still be that nonlinearities arise because individual thresholds in the presence of noise might depend on the variable amplitude of noise applied to different participants, since noise intensities were proportional to the individual baseline thresholds, which were also quite variable (see above). The results with the highest noise level (k = 2) are especially critical in this respect, since the performance at this level discriminates between non-monotonic (SR-like) and monotonic behaviors, as mentioned above.

In Fig. 6, we plotted the ratio of individual threshold values obtained at the nominal noise level of k = 2 relative to baseline thresholds as a function of the actual values of noise measured in each participant. Contrary to the prediction that individual threshold values depend on the specific noise acceleration, the linear regression was flat (−0.011 slope, P = 0.79), and the intercept was close to 1 (0.96 intercept) consistent with the previous observation that the threshold at k = 2 was close to baseline thresholds (see above). The individual

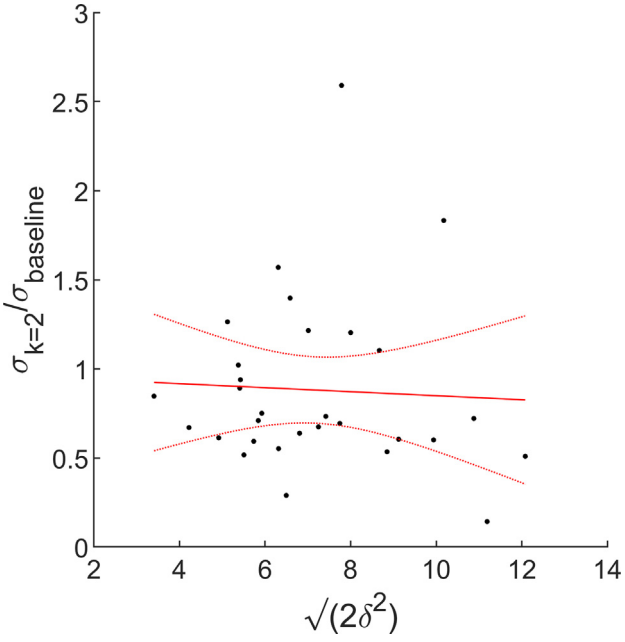

Fig. 6. Scatter plot of the ratio of individual threshold values at the nominal noise level of k = 2 relative to baseline thresholds vs the actual values of noise measured in each participant. Solid and dotted lines represent the linear regression fit and the 95% confidence bounds, respectively.

threshold values did not significantly depend on the specific noise acceleration also for the other levels of noise (k = 0.5, 1 and 1.5, all P > 0.06).

DISCUSSION

We applied small-amplitude motion perturbations during a motion discrimination task at different levels of noise. At the population level, we found that the thresholds for all but the highest level of noise were significantly lower than the baseline threshold. At the individual level, the threshold was lower with at least one noise level than the threshold without noise in 87% of the participants. We suggest that noisy mechanical oscillations of the whole body can increase the probability of recognizing the direction of motion from low, normally subthreshold vestibular signals, possibly due to stochastic resonance (SR) effects.

Threshold values

With the noise conditions, we randomly interspersed a control with zero noise to verify the consistency of the baseline threshold estimate. At the population level, we found no statistically significant difference of threshold between the control and the baseline. This result is consistent with previous reports showing limited session-to-session, intra-subject variability of the vestibular motion discrimination thresholds (Hartmann et al., 2013; Clark et al., 2018; Wagner et al., 2022). On the other hand, we found large inter-subject variability of the thresholds both in the unperturbed conditions (baseline and control) and in the noise conditions. Inter-subject variability of motion discrimination thresholds has also been reported in previous studies (Guedry, 1974; Bermúdez Rey et al., 2016; Diaz-Artiles and Karmali, 2021).

As for the absolute values of the motion thresholds, these may not be easily comparable across different studies because of methodological and individual differences (Diaz-Artiles and Karmali, 2021). Nevertheless, the average motion thresholds we found are close to those reported for naso-occipital translations by Benson et al. (1986), Greig (1988), Naseri and Grant (2012), Agrawal et al. (2013), and Bremova et al. (2016). However, they are higher than those reported by Kobel et al. (2021).

We found that participants with higher thresholds in the unperturbed conditions benefitted more (i.e., showed greater threshold improvements) from added noise than participants with lower unperturbed thresholds. This result reminds of the previous observation that individuals with worse baseline ocular counter-rolling gain (a vestibular-mediated response) demonstrated the greatest improvements (increases in gain) with galvanic vestibular stimulation (Serrador et al., 2018).

Stochastic resonance

Stochastic resonance (SR) is a nonlinear phenomenon whereby the addition of a random interference (noise) can enhance the detection of weak stimuli or the information content of the signal (Moss et al., 2004). An optimal amount of added noise results in the maximum enhancement and further increases in the noise intensity do not lead to any enhancement. Accordingly, the signature of SR is a pseudo-bell shape curve with a peak in performance at some noise level associated with optimal system output (Moss et al., 2004). The present results are qualitatively compatible with the presence of SR at the population level: on average, the thresholds at low to intermediate levels of noise were significantly lower than the baseline threshold, while the threshold at the highest level of noise was not significantly different from the baseline (Fig. 5).

This average trend with noise level rules out a simpler explanation involving a superposition of noise and stimulus. For any given test stimulus, as the amplitude of noise increases, the peak acceleration of the overall input (stimulus plus noise) increases proportionally to noise. Therefore, if the reduction in threshold depended on an increase of peak acceleration (without the necessity of invoking the non-linearity of SR), one would expect that the threshold at the highest level of noise (k = 2) should be further reduced relative to lower levels of noise, the opposite of what we found. Moreover, we found that the ratio of individual threshold values obtained at each nominal level of noise relative to baseline thresholds did not vary significantly with the actual values of noise measured in each participant (Fig. 6), again running contrary to the hypothesis that a linear combination of noise and stimulus boosts the responses in proportion to the amplitude of noise.

SR-like effects were observed at the population level, but they were not consistent from subject to subject. Indeed, a clear pseudo-bell shape curve was present only in a subset of subjects (Fig. 4). Moreover, one should consider that the trends of motion discrimination thresholds as a function of motion amplitude may depend on multiple factors. In addition to potential SR effects, neural variability may contribute substantially to perceptual performance. Indeed, neural discrimination thresholds tend to saturate for higher stimulus amplitudes (Carriot et al., 2021), which is a trend comparable to that previously observed for vestibular perception leading to violations of Weber's law (Mallery et al., 2010; Naseri and Grant, 2012). This may account for the observation that the thresholds at the highest noise level (k = 2) were not significantly different from the baseline, but not as much degraded as one may expect from a strict SR behavior.

In sum, vestibular motion discrimination can be enhanced by small-amplitude whole-body noise. However, the hypothesis that this occurs through SR mechanisms, although plausible, remains to be further verified against alternative hypotheses.

Comparison with GVS studies

When comparing the present results with previous results obtained using stochastic galvanic vestibular stimulation, one should consider that whole-body mechanical oscillations engage the vestibular system in a very different manner relative to the trans-mastoid electrical

stimulation of GVS. First, vestibular responses to whole-body oscillations are mediated by head and body biomechanics, whereas GVS bypasses both the body biomechanics and the mechano-transduction of semicircular canals and otolith organs, directly stimulating the hair cells and vestibular afferents (Kwan et al., 2019; Dlugaiczyk et al., 2019). Second, the mechanical oscillations of the present experiments were applied roughly along a nano-occipital axis, whereas bilateral bipolar GVS has been shown to evoke responses mainly along an inter-aural axis (Fitzpatrick and Day, 2004; Dlugaiczyk et al., 2019). In fact, it has been argued that, since GVS induces simultaneous activation of primary afferents from all vestibular sensory end organs on one side with concomitant inhibition of those on the contralateral side, the resulting stimulation pattern has no physiological motion equivalent (Kwan et al., 2019).

Despite these limitations in the comparison, the global trends reported in previous GVS studies of motion discrimination (Galvan-Garza et al., 2018; Keywan et al., 2018, 2019, 2020a) are qualitatively similar to those we found here. Thus, both GVS studies and our study found lower vestibular motion thresholds with noise than without noise. Similarly to our results, improvements in vestibular thresholds associated with GVS were found within the subject pool, but they were not consistent from subject to subject (Galvan-Garza et al., 2018; Keywan et al., 2018, 2019, 2020a; Voros et al., 2021). Also, the optimal stimulus intensity yielding the largest reduction of threshold could differ substantially across subjects, as was the case in the present study. Finally, for both GVS and our stimuli, the trends with noise intensity were consistent with SR effects only in a subset of subjects.

Putative substrates

We tested motion discrimination in the antero-posterior direction. While this direction roughly corresponded to the naso-occipital axis, we did not check the exact alignment with this axis. Moreover, we measured some (small) variability in head orientation across experiments, which was expected since the head was not rigidly fixed relative to the platform.

Translations along the naso-occipital axis mainly assess utricular function, but also engage the saccules to some extent (Kobel et al., 2021). Studies have demonstrated that vestibular cues predominate for the perception of motion direction in blindfolded subjects, proprioceptive and tactile cues from the motion platform being absent or minimal (Chaudhuri et al., 2013; Valko et al., 2012). On the other hand, the small-amplitude noise we added to the translations generated vibrations that presumably affected multiple vestibular and non-vestibular (e.g., skin, muscle, visceral) receptors. While humans are extremely sensitive to minute vibrations (Parsons and Griffin, 1988), it has been argued convincingly that, in line of principle, vibrations can contribute to motion detection but not to motion direction discrimination tasks (Merfeld, 2011; Chaudhuri et al., 2013). Indeed, a discrimination task would be affected by vibration cues only if subjects were able to distinguish some asymmetry in the vibration for forward motion versus the vibration for backward motion (Chaudhuri et al., 2013). Here, given the symmetrical nature of the applied noise, subjects could not extract directional information from the noise *per se*. However, our results indicate that the energy and information carried by the noise were combined with those of subthreshold motion stimuli, thus lowering the thresholds of direction discrimination for some levels of noise. Specifically, our lower amplitude noisy perturbations ($k = 0.5, 1, 1.5$) boosted the vestibular signals presumably by facilitating the threshold crossing, without excessive distortion of the sinusoidal stimulus (see Fig. 1). When the amplitude of the noise was higher ($k = 2$), however, noisy oscillations crossed the threshold but also distorted the stimulus considerably, thus confounding motion discrimination.

If one considers the hypothesis of stochastic resonance as a tentative explanation of the present results, one may surmise that the frequencies in the band-limited white noise resonate with critical frequencies of vestibular signals elicited by the primary motion stimulus, amplifying the original signal and increasing the signal-to-noise ratio at neural processing stages (Rouvas-Nicolis and Nicolis, 2007). The added noise can be sufficient to make the signal detectable by the vestibular sensors, and then it can be filtered out so as to discriminate the original, previously unrecognizable signal.

Otolith receptors in the maculae are extremely sensitive, being able to detect displacements of the cilia at atomic scales and correspondingly small accelerations (Howard and Hudspeth, 1988). In the maculae, the striola band consists of mainly type I receptors whose hair bundles are weakly tethered to the overlying otolithic membrane. The afferent neurons have irregular resting discharge and have low thresholds to high frequency bone-conducted vibration (Young et al., 1977; Curthoys et al., 2017). We surmise that irregular afferents may mediate SR-like effects due to small vibrations. In a similar vein, it has been suggested that Brownian motion of the hair bundle of the inner hair cells of the cochlea serves to enhance the sensitivity of mechanoelectrical transduction (Jaramillo and Wiesenfeld, 1998). Of course, our study cannot shed any light on the neural mechanisms involved in SR-like effect. With regards to GVS, for instance, it has been shown in the monkey that, despite the lower sensitivity of regular afferents to such stimuli compared to irregular afferents, they transmit equivalent information to central vestibular pathways for the detection of GVS-evoked sensations of self-motion (Kwan et al., 2019).

Limitations

As a first attempt to quantify the effects of small perturbations on the motion direction discrimination, our study has limitations that could be remedied in future studies. First, because of the constraints on overall testing time (due to COVID-19 regulations at our Institution), we only investigated the effects of noise on vestibular motion discrimination in the antero-posterior direction. Moreover, we applied noise in the same direction as the motion stimuli to be discriminated. We

do not know whether perceptual enhancements would still be obtained with noise applied in a direction different from that of the motion stimuli. For instance, prolonged conditioning stimuli consisting of subliminal interaural translations reduced the thresholds not only for motion discrimination in the same direction but also in the naso-occipital direction (Keywan et al., 2020b, 2022). However, these conditioning stimuli did not affect significantly the thresholds for yaw rotations (Keywan et al., 2020b), indicating some selectivity for the otoliths. We only used four levels of non-zero noise, again due to the constraints in testing time. The ability to detect a clear-cut U-shaped function as a function of applied noise (the hallmark of SR) strongly depends on the application of several noise levels (Moss et al., 2004; McDonnell and Abbott, 2009; Galvan-Garza, 2016).

Our study provides initial evidence that small-amplitude motion perturbations can enhance the perceptual discrimination of motion direction. The results, though not directly comparable, are reminiscent of previous results obtained with stochastic galvanic vestibular stimulation (Galvan-Garza et al., 2018; Keywan et al., 2018, 2019, 2020a), and extend the conclusions to more natural vestibular stimuli. Our results have further potential implications for both physiology and medicine. From a physiological standpoint, the results suggest the possibility that, just as the external noise that we applied, also the small, spontaneous random oscillations of the body associated with standing posture and other daily activities (Duarte and Zatsiorsky, 2000; Carriot et al., 2014; Fino et al., 2020) are beneficial by enhancing vestibular thresholds with a mechanism similar to SR. If this was the case, the perceptual precision of head motion discrimination and spatial orientation would be increased during challenging conditions. From a clinical standpoint, there is the possibility that the application of small-amplitude motion perturbations can be a useful rehabilitation tool for individuals with elevated thresholds for vestibular motion perception, such as people with vestibulopathy (Eder et al., 2022), vestibular hypofunction (Priesol et al., 2014) or the elderly (Bermúdez Rey et al., 2016). In this respect, it remains to be seen whether noise such as that we applied here can improve not just vestibular perception, but also vestibulo-spinal function for balance control. This has been shown to be the case for GVS (Mulavara et al., 2011).

AUTHORS CONTRIBUTIONS

All authors designed the experiments, analyzed the results, and wrote the paper.

DECLARATIONS OF INTEREST

None.

ACKNOWLEDGMENTS

We thank Claudia Brunetti, Giorgio Capuzzi, Alessia Celli and Greta Dimasi for help with the setup and experiments. This work was supported by the Italian Ministry of Health (Ricerca corrente, IRCCS Fondazione Santa Lucia, Ricerca Finalizzata RF-2018-12365985), Italian Space Agency (grant I/006/06/0 and grant 2019-11-U.0), INAIL (BRIC 2019), and Italian University Ministry (PRIN grant 20208RB4N9_002 and 2020EM9A8X_003).

Participants gave written informed consent to procedures approved by the Institutional Review Board of Santa Lucia Foundation (protocol n. CE/PROG.757), in conformity with the Declaration of Helsinki (World Medical Association, 2013) regarding the use of human participants in research.

REFERENCES

Agrawal Y, Bremova T, Kremmyda O, Strupp M, MacNeilage PR (2013) Clinical testing of otolith function: perceptual thresholds and myogenic potentials. J Assoc Res Otolaryngol 14 (6):905–915.

Angelaki DE, Cullen KE (2008) Vestibular system: the many facets of a multimodal sense. Annu Rev Neurosci 31(1):125–150.

Benson AJ, Spencer MB, Stott JRR (1986) Thresholds for the detection of the direction of whole-body, linear movement in the horizontal plane. Aviat Space Environ Med 57:1088–1096.

Benzi R, Parisi G, Sutera A, Vulpiani A (1982) Stochastic resonance in climatic change. Tellus 34:10–16.

Bermúdez Rey MC, Clark TK, Wang W, Leeder T, Bian Y, Merfeld DM (2016) Vestibular perceptual thresholds increase above the age of 40. Front Neurol 7:162.

Bremova T, Caushaj A, Ertl M, Strobl R, Böttcher N, Strupp M, MacNeilage PR (2016) Comparison of linear motion perception thresholds in vestibular migraine and Menière's disease. Eur Arch Otorhinolaryngol 273:2931–2939.

Carriot J, Cullen KE, Chacron MJ (2021) The neural basis for violations of Weber's law in self-motion perception. PNAS 118 (36).

Carriot J, Jamali M, Chacron MJ, Cullen KE (2014) Statistics of the vestibular input experienced during natural self-motion: implications for neural processing. J Neurosci 34(24):8347–8357.

Chaudhuri SE, Karmali F, Merfeld DM (2013) Whole body motion-detection tasks can yield much lower thresholds than direction-recognition tasks: implications for the role of vibration. J Neurophysiol 110:2764–2772.

Chaudhuri SE, Merfeld DM (2013) Signal detection theory and vestibular perception: III. Estimating unbiased fit parameters for psychometric functions. Exp Brain Res 225:133–146.

Clark TK, Merfeld DM (2021) Statistical approaches to identifying lapses in psychometric response data. Psychon Bull Rev 28 (5):1433–1457.

Clark TK, Yi Y, Galvan-Garza RC, Bermudez Rey MC, Merfeld DM (2018) When uncertain, does human self-motion decision-making fully utilize complete information? J Neurophysiol 119:1485–1496.

Collins JJ, Imhoff TT, Grigg P (1996a) Noise-enhanced information transmission in rat SA1 cutaneous mechanoreceptors via aperiodic stochastic resonance. J Neurophysiol 76:642–645.

Collins JJ, Imhoff TT, Grigg P (1996b) Noise-enhanced tactile sensation. Nature 383:770.

Cordo P, Inglis JT, Verschueren S, Collins JJ, Merfeld DM, Rosenblum S, Buckley S, Moss F (1996) Noise in human muscle spindles. Nature 383:769–770.

Crane BT (2012) Fore-aft translation aftereffects. Exp Brain Res 219:477–487.

Curthoys IS, MacDougall HG, Vidal P-P, de Waele C (2017) Sustained and Transient Vestibular Systems: A Physiological Basis for Interpreting Vestibular Function. Front Neurol 8:117.

Dhawale AK, Smith MA, Ölveczky BP (2017) The role of variability in motor learning. Annu Rev Neurosci 40:479–498.

Diaz-Artiles A, Karmali F (2021) Vestibular precision at the level of perception, eye movements, posture, and neurons. Neuroscience 468:282–320.
Dlugaiczyk J, Gensberger KD, Straka H (2019) Galvanic vestibular stimulation: from basic concepts to clinical applications. J Neurophysiol 121:2237–2255.
Duarte M, Zatsiorsky VM (2000) On the fractal properties of natural human standing. Neurosci Lett 283(3):173–176.
Eder J, Kellerer S, Amberger T, Keywan A, Dlugaiczyk J, Wuehr M, Jahn K (2022) Combining vestibular rehabilitation with noisy galvanic vestibular stimulation for treatment of bilateral vestibulopathy. J Neurol 269:5731–5737.
Faisal AA, Selen LPJ, Wolpert DM (2008) Noise in the nervous system. Nat Rev Neurosci 9:292–303.
Fino PC, Raffegeau TE, Parrington L, Peterka RJ, King LA (2020) Head stabilization during standing in people with persisting symptoms after mild traumatic brain injury. J Biomech 112 110045.
Fitzpatrick RC, Day BL (2004) Probing the human vestibular system with galvanic stimulation. J Appl Physiol 96:2301–2316.
Flores A, Manilla S, Huidobro N, De la Torre-Valdovinos B, Kristeva R, Mendez-Balbuena I, Galindo F, Trevino M, Manjarrez E (2016) Stochastic resonance in the synaptic transmission between hair cells and vestibular primary afferents in development. Neuroscience 322:416–429.
Fujimoto C, Yamamoto Y, Kamogashira T, Kinoshita M, Egami N, Uemura Y, Togo F, Yamasoba T, Iwasaki S (2016) Noisy galvanic vestibular stimulation induces a sustained improvement in body balance in elderly adults. Sci Rep 6(1):1–8.
Galvan-Garza R (2016) Enhancement of perception with the application of stochastic vestibular stimulation. Massachusetts Institute of Technology. PhD Thesis..
Galvan-Garza RC, Clark TK, Mulavara AP, Oman CM (2018) Exhibition of stochastic resonance in vestibular tilt motion perception. Brain Stimul 11:716–722.
Gammaitoni L, Hanggi P, Jung P, Marchesoni F (1998). Stochastic resonance. Rev Mod Phys 70:223–288.
Goel R, Kofman I, Jeevarajan J, De Dios Y, Cohen HS, Bloomberg JJ, Mulavara AP (2015) Using low levels of stochastic vestibular stimulation to improve balance function. PLoS One 10(8): e0136335.
Grabherr L, Nicoucar K, Mast FW, Merfeld DM (2008) Vestibular thresholds for yaw rotation about an earth-vertical axis as a function of frequency. Exp Brain Res 186:677–681.
Greig GL (1988) Masking of motion cues by random motion: comparison of human performance with a signal detection model. UTIAS (University of Toronto). Report 313,.
Guedry FE (1974) Psychophysics of vestibular sensation. In: Vestibular system. Part 2: psychophysics, applied aspects and general interpretations. Berlin, Heidelberg, New York: Springer-Verlag. p. 3–154.
Hartmann M, Furrer S, Herzog MH, Merfeld DM, Mast FW (2013) Self-motion perception training: thresholds improve in the light but not in the dark. Exp Brain Res 226:231–240.
Hirasaki E, Moore ST, Raphan T, Cohen B (1999) Effects of walking velocity on vertical head and body movements during locomotion. Exp Brain Res 127(2):117–130.
Howard J, Hudspeth AJ (1988) Compliance of the hair bundle associated with gating of mechanoelectrical transduction channels in the bullfrog's saccular hair cell. Neuron 1(3): 189–199.
Iwasaki S, Yamamoto Y, Togo F, Kinoshita M, Yoshifuji Y, Fujimoto C, Yamasoba T (2014) Noisy vestibular stimulation improves body balance in bilateral vestibulopathy. Neurology 82:969–975.
Iwasaki S, Fujimoto C, Egami N, Kinoshita M, Togo F, Yamamoto Y, Yamasoba T (2018) Noisy vestibular stimulation increases gait speed in normals and in bilateral vestibulopathy. Brain Stimul 11 (4):709e15.
Jaramillo F, Wiesenfeld K (1998) Mechanoelectrical transduction assisted by Brownian motion: a role for noise in the auditory system. Nat Neurosci 1:384–388.
Kabbaligere R, Layne CS, Karmali F (2018) Perception of threshold-level whole-body motion during mechanical mastoid vibration. J Vestib Res 28(3–4):283–294.
Karmali F, Lim K, Merfeld DM (2014) Visual and vestibular perceptual thresholds each demonstrate better precision at specific frequencies and also exhibit optimal integration. J Neurophysiol 111:2393–2403.
Karmali F, Chaudhuri SE, Yi Y, Merfeld DM (2016) Determining thresholds using adaptive procedures and psychometric fits: evaluating efficiency using theory, simulations, and human experiments. Exp Brain Res 234:773–789.
Karmali F, Goodworth AD, Valko Y, Leeder T, Peterka RJ, Merfeld DM (2021) The role of vestibular cues in postural sway. J Neurophysiol 125:672–686.
Keywan A, Wuehr M, Pradhan C, Jahn K (2018) Noisy galvanic stimulation improves roll-tilt vestibular perception in healthy subjects. Front Neurol 9:83.
Keywan A, Jahn K, Wuehr M (2019) Noisy galvanic vestibular stimulation primarily affects otolith-mediated motion perception. Neuroscience 399:161–166.
Keywan A, Badarna H, Jahn K, Wuehr M (2020a) No evidence for after-effects of noisy galvanic vestibular stimulation on motion perception. Sci Rep 10(1):1–7.
Keywan A, Dietrich H, Wuehr M (2020b) Subliminal passive motion stimulation improves vestibular perception. Neuroscience 441:1–7.
Keywan A, Yassin G, Jahn K, Wuehr M (2022) Subliminal conditioning of vestibular perception generalizes within otolith organs. J Neurol 269(10):5258–5261.
Kingma H (2005) Thresholds for perception of direction of linear acceleration as a possible evaluation of the otolith function. BMC Ear Nose Throat Disord 5(1):1–6.
Kobel MJ, Wagner AR, Merfeld DM (2021) Impact of gravity on the perception of linear motion. J Neurophysiol 126:875–887.
Kwan A, Forbes PA, Mitchell DE, Blouin JS, Cullen KE (2019) Neural substrates, dynamics and thresholds of galvanic vestibular stimulation in the behaving primate. Nat Commun 10(1):1–15.
Leek MR (2001) Adaptive procedures in psychophysical research. Percept Psychophys 63:1279–1292.
Mallery RM, Olomu OU, Uchanski RM, Militchin VA, Hullar TE (2010) Human discrimination of rotational velocities. Exp Brain Res 204:11–20.
Martínez L, Pérez T, Mirasso CR, Manjarrez E (2007) Stochastic resonance in the motor system: effects of noise on the monosynaptic reflex pathway of the cat spinal cord. J Neurophysiol 97:4007–4016.
McDonnell MD, Abbott D (2009) What is stochastic resonance? Definitions, misconceptions, debates, and its relevance to biology. PLoS Comput Biol 5(5):e1000348.
Merfeld DM (2011) Signal detection theory and vestibular thresholds: I. Basic theory and practical considerations. Exp Brain Res 210 (3):389–405.
Merfeld DM (2012) Spatial orientation and the vestibular system. In: Carroll S, editor. Sensation and Perception. Sunderland, MA: Sinauer Associates. p. 328–361.
Mitchell DE, Kwan A, Carriot J, Chacron MJ, Cullen KE (2018) Neuronal variability and tuning are balanced to optimize naturalistic self-motion coding in primate vestibular pathways. Elife 7:e43019.
Mori T, Kai S (2002) Noise-induced entrainment and stochastic resonance in human brain waves. Phys Rev Lett 88(21) 218101.
Moscatelli A, Mezzetti M, Lacquaniti F (2012) Modeling psychophysical data at the population-level: the generalized linear mixed model. J Vis. 12(11).
Moss F, Ward LM, Sannita WG (2004) Stochastic resonance and sensory information processing: a tutorial and review of application. Clin Neurophysiol 115:267–281.
Mulavara AP, Fiedler MJ, Kofman IS, Wood SJ, Serrador JM, Peters B, Cohen HS, Reschke MF, Bloomberg JJ (2011) Improving balance function using vestibular stochastic resonance: optimizing stimulus characteristics. Exp Brain Res 210:303–312.

Mulavara AP, Kofman IS, De Dios YE, Miller C, Peters BT, Goel R, et al. (2015) Using low levels of stochastic vestibular stimulation to improve locomotor stability. Front Syst Neurosci 9:117.
Naseri AR, Grant PR (2012) Human discrimination of translational accelerations. Exp Brain Res 218:455–464.
Nooristani M, Bigras C, Lafontaine L, Bacon BA, Maheu M, Champoux F (2021) Vestibular function modulates the impact of nGVS on postural control in older adults. J Neurophysiol 125:489–495.
Parsons KC, Griffin MJ (1988) Whole-body vibration perception thresholds. J Sound Vib 121:237–258.
Pozzo T, Berthoz A, Lefort L (1990) Head stabilization during various locomotor tasks in humans: I. Normal subjects. Exp Brain Res 82 (1):97–106.
Priesol AJ, Valko Y, Merfeld DM, Lewis RF (2014) Motion perception in patients with idiopathic bilateral vestibular hypofunction. Otolaryngol Head Neck Surg 150(6):1040–1042.
Putman EJ, Galvan-Garza RC, Clark TK (2021) The Effect of Noisy Galvanic Vestibular Stimulation on Learning of Functional Mobility and Manual Control Nulling Sensorimotor Tasks. Front Hum Neurosci 15 756674.
Roditi RE, Crane BT (2012) Directional asymmetries and age effects in human self-motion perception. J Assoc Res Otolaryngol 2012 (13):381–401.
Rodriguez R, Crane BT (2018) Effect of vibration during visual-inertial integration on human heading perception during eccentric gaze. PLoS One 13(6):e0199097.
Rouvas-Nicolis C, Nicolis G (2007) Stochastic resonance. Scholarpedia 2:1474. https://doi.org/10.4249/scholarpedia.1474.
Serrador JM, Deegan BM, Geraghty MC, Wood SJ (2018) Enhancing vestibular function in the elderly with imperceptible electrical stimulation. Sci Rep 8(1):336.
Simonotto E, Riani M, Seife C, Roberts M (1997) Visual perception of stochastic resonance. Phys Rev Lett:256:6e9.
Stefani SP, Serrador JM, Breen PP, Camp AJ (2020) Impact of galvanic vestibular stimulation-induced stochastic resonance on the output of the vestibular system: A systematic review. Brain Stimul 13(3):533–535.
Taylor M, Creelman CD (1967) PEST: Efficient estimates on probability functions. J Acoust Soc Am 41:782–787.
Treviño M, De la Torre-Valdovinos B, Manjarrez E (2016) Noise improves visual motion discrimination via a stochastic resonance-like phenomenon. Front. Hum. Neurosci. 10:572.
Tukey JW (1958) Bias and Confidence in Not-Quite Large Samples. Front. Hum. Neurosci. 29(2):614.
Utz KS, Korluss K, Schmidt L, Rosenthal A, Oppenländer K, Keller I, Kerkhoff G (2011) Minor adverse effects of galvanic vestibular stimulation in persons with stroke and healthy individuals. Brain Inj 25:1058–1069.
Valko Y, Lewis RF, Priesol AJ, Merfeld DM (2012) Vestibular labyrinth contributions to human whole-body motion discrimination. J Neurosci 32:13537–13542.
van der Groen O, Wenderoth N (2016) Transcranial random noise stimulation of visual cortex: stochastic resonance enhances central mechanisms of perception. J Neurosci 36:5289–5298.
Vidal PP, Lacquaniti F (2021) Perceptual-motor styles. Exp Brain Res 239(5):1359–1380.
Voros JL, Sherman SO, Rise R, Kryuchkov A, Stine P, Anderson AP, Clark TK (2021) Galvanic Vestibular Stimulation Produces Cross-Modal Improvements in Visual Thresholds. Front Neurosci 15:640984.
Wagner AR, Kobel MJ, Tajino J, Merfeld DM (2022) Improving self-motion perception and balance through roll tilt perceptual training. J Neurophysiol 128(3):619–633.
Wang L, Zobeiri OA, Millar JL, Souza Silva W, Schubert MC, Cullen KE (2021) Continuous Head Motion is a Greater Motor Control Challenge than Transient Head Motion in Patients with Loss of Vestibular Function. Neurorehabil Neural Repair 35(10):890–902.
Wells C, Ward LM, Chua R, Inglis JT (2005) Touch noise increases vibrotactile sensitivity in old and young. Psychol Sci 16:313–320.
World Medical Association (2013) World Medical Association Declaration of Helsinki: ethical principles for medical research involving human subjects. J Am Med Assoc 310:2191–2194.
Wuehr M, Boerner JC, Pradhan C, Decker J, Jahn K, Brandt T, Schniepp R (2018) Stochastic resonance in the human vestibular system – Noise-induced facilitation of vestibulospinal reflexes. Brain Stimul 11:261–263.
Yashima J, Kusuno M, Sugimoto E, Sasaki H (2021) Auditory noise improves balance control by cross-modal stochastic resonance. Heliyon 7(11):e08299.
Young ED, Fernandez C, Goldberg JM (1977) Responses of squirrel monkey vestibular neurons to audio-frequency sound and head vibration. Acta Otolaryngol 84(5–6):352–360.
Zink R, Bucher SF, Weiss A, Brandt T, Dieterich M (1998) Effects of galvanic vestibular stimulation on otolithic and semicircular canal eye movements and perceived vertical. Electroencephalogr. clin. neurophysiol. 107(3):200–205.

GLOSSARY

3D: three-dimensional
BRGLM: bias-reduced generalized linear model
95% CI: confidence interval at 95%
GLM: general linear model
GLMM: Generalized Linear Mixed Model
GVS: galvanic vestibular stimulation
LIA: lapse-identification algorithm
RM-ANOVA: Repeated measures analysis of variance
SD: standard deviation
SR: stochastic resonance

(Received 17 August 2022, Accepted 10 December 2022)
(Available online 16 December 2022)